

Resorbable magnesium scaffolds for coronary vascular intervention; From bench to clinics

Dr. Thomas Hefti and Mrs. Philine Baumann-Zumstein
Biotronik AG, Vascular Interventions, Bülach, Switzerland

INTRODUCTION: Resorbable vascular scaffolds have the potential to overcome the remaining limitations of permanent drug eluting stents by allowing vascular restoration over time. Amongst the current clinically tested resorbable materials, magnesium based devices, such as Magmaris (BIOTRONIK AG, Bülach, Switzerland) appear to have promising properties to achieve good and safe clinical results.

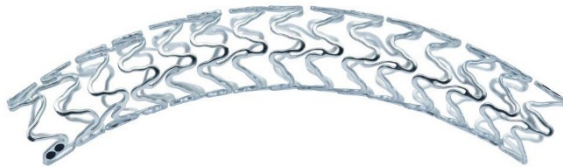


Fig. 1: Magmaris resorbable magnesium scaffold

METHODS: In vitro bench testing included deliverability, magnesium scaffold expansion behaviour with acute elastic and time dependent recoil and radial strength in comparison to polymer based scaffolds.

In vivo preclinical animal studies evaluated device safety and performance and characterized key scaffold features such as pharmacokinetics and degradation mechanism / kinetics.

Clinical safety and performance was assessed in multiple studies with primary endpoints such as in-segment late lumen loss at 6 months (BIOSOLVE II), in hospital procedural success (BIOSOLVE-III) or target lesion failure at 12 months in real world setting (BIOSOLVE-IV).

RESULTS: The magnesium alloy used for Magmaris exhibits improved mechanical strength as compared to polymeric based scaffolds. Bench testing revealed a strong radial resistance and reduced recoil behaviour both in acute and in time dependent settings as well as improved deliverability [1].

Preclinical in vivo results suggest a retarded drug elution profile with an encouraging safety profile with advanced healing, low acute thrombogenicity and reduction of neo-atherosclerosis [2,3,4,5]. At 1 year after implantation, a majority of the magnesium was resorbed and replaced by an amorphous calcium phosphate, accompanied by a rapid increase in strut discontinuity density between 28 days and 1 year [6].

First-in-man and pivotal clinical trials demonstrated favourable safety profiles with significantly improved late lumen loss at 6 months compared to the precursor devices as well as low target lesion failure and target lesion revascularization rates with no definite or probable scaffold thrombosis up to 36 months [7,8]. Post market observational registry confirmed low TLF rates of previous studies and very good overall safety profile up to 12 months [9].

DISCUSSION & CONCLUSIONS: Overall, resorbable vascular scaffolds made out of magnesium alloys show promising *in vitro*, *in vivo* and clinical results.

REFERENCES:

- ¹ W. Schmidt et al. *Cardiovasc Revasc Med.* 2016 Sep; **17**(6):375-83.
- ² R. Waksman et al. *EuroIntervention.* 2017 Jul 20; **13**(4):440-449.
- ³ R. Waksman et al. *Circ Cardiovasc Interv.* 2017 Aug; **10**(8).
- ⁴ M.J. Lipinski, et al. *EuroIntervention.* 2019 Jan 20; **14**(13).
- ⁵ M. Joner. Presented at: ESC; Aug 28, 2017; Barcelona, Spain.
- ⁶ M. Joner, et al. *EuroIntervention.* 2018 Oct 12; **14**(9).
- ⁷ M. Haude et al. *Lancet.* 2016 Jan 2; **387** (10013):31-9.
- ⁸ M. Haude et al. *EuroIntervention.* 2019 Feb 26.
- ⁹ Verheye et al. *EuroIntervention.* 2019 Jan 22.

Galvanic corrosion of magnesium materials

H Hornberger¹, J Wolker¹, H Kissel¹

¹ *Biomaterials Lab, Faculty of Mechanical Engineering, University of applied Science OTH Regensburg, Germany*

INTRODUCTION: Ions will be dissolved on the surface of metallic implant materials due to electrochemical corrosion processes [1], which can interact with host tissue [2]. If permanent implants are applied, the corrosion resistance is very high and the corrosion rate as low as possible. However, using resorbable implant materials, higher corrosion rates are necessary to allow degradation. The control of this corrosion rate implies that the implant will be mechanically stable after implantation as long as needed for remodelling but on the other side the complete degradation of the implant is supposed to take place in a determined time period. Magnesium is chemically reactive because the electrochemical potential is very low. In contact with other metallic materials, magnesium will preferentially take over the role of the sacrificial anode. That means that for example an implanted osteosynthesis plate might be combined with a magnesium alloy screw within the body. Then galvanic corrosion takes place and increases the total corrosion velocity due to the summation of self-induced and galvanic current:

$$I_{total} = I_{self-induced} + I_{galvanic} \quad (1)$$

The self-induced corrosion current is for the surface of magnesium materials mostly due to micro-galvanic corrosion. The aim of this study was to evaluate the enhanced corrosion behavior due to galvanic corrosion effects.

METHODS: Immersion studies were performed on magnesium alloys AM50 and WE43, the hydrogen evolution was used to evaluate corrosion rates [3]. Contact partner were Ti cp2 and 316L samples as typical implant materials, electrolytes 0.9% NaCl as well as buffered solution. The sample was prepared as shown in Fig. 1 to allow careful polishing to roughness values of about 0.02 μm . Various area proportions were applied (1:1, 1:4 and 4:1) and the corrosion rates determined. Additionally some ZRA measurements were performed to estimate the galvanic part of the corrosion occurring.

RESULTS & DISCUSSION: The results of both methods showed that higher corrosion takes place if the area correlation anode : cathode = 1:4 compared with an applied area correlation of 4:1, the increase was about 50% using titanium a contact partner. That confirms that using a larger cathodic area, the consumption of electrons produced by the anodic corrosion reaction, and thus the anodic corrosion is enhanced. Using a smaller cathodic surface area the galvanic corrosion current is limited. Additionally, the stainless steel 316L as the contact partner had a higher impact than expected. ZRA measurements were accompanied with high deviation, thus it was not yet possible to determine the galvanically caused part of corrosion. The measured current was in the range of mA/cm^2 , which is similar to values of another study [4].

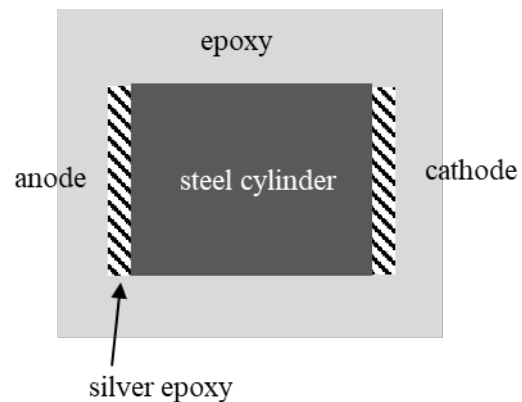


Fig. 1: Galvanic corrosion samples for immersion test

REFERENCES: ¹W.-D. Mueller and H. Hornberger (2014) *Int J Mol Sci* **15**:11456-11472. ²Y.F. Zheng, X.N. Gu, F. Witte (2014) *Mater Sci Eng* **R77**:1-34. ³G. Song, A. Atrens and D. StJohn (2001) An hydrogen evolution method for the estimation of the corrosion rate of magnesium alloy, in *Magnesium Technology TMS* (ed J.N. Hryn) 255-262. ⁴M. Mohedano, R. Arrabal, A. Pardo et al. (2014) *Revista de Metalurgia* **50**: 1, 9 pages.

Fixation of a mandible osteotomy with magnesium implants: Does transferability to humans depend on the miniature pig breed?

T Imwinkelried¹, S Beck², B Schaller³

¹ RMS Foundation, Bettlach, CH, ² Synthes Biomaterials, Oberdorf, CH, ³ Department of Cranio-Maxillofacial Surgery, University Hospital, Bern, CH

INTRODUCTION: Skeletally mature miniature pigs were used as an animal model to investigate human sized magnesium implants. A mandible osteotomy was treated using human-like surgical techniques for the osteosynthesis.

METHODS: A pilot study with two Göttingen minipigs (University Hospital Bern, Switzerland) and a subsequent performance study with seven Yucatan minipigs (AccelLAB, Boisbriand, Canada) were carried out. A full osteotomy of the mandible was inflicted with an oscillating saw next to the mandibular angle. Two locking plates with four holes were used for the osteosynthesis (Figure 1): a thinner plate with monocortical screws (M) and a thicker plate with bicortical screws (B). Commercially available cp Ti plates and Ti-Al-Nb screws served as a control. A material specific design was used for the magnesium implants to achieve equivalent bending stiffness and strength. Plate thicknesses and screw diameters were increased by a factor ~1.5 compared to titanium. The screw drives had a build-in torque limiting feature.

A magnesium alloy based on the composition of WE43 (Mg-Y-Nd-RE), but with a lower impurity level was used (Magnesium Elektron, Swinton, England). A plasma-electrolytic, magnesium phosphate coating with ~10 µm thickness was applied. The locking threads were not coated to allow electrochemical continuity.

RESULTS: The pilot study with the two Göttingen minipigs was promising. The X-ray computed tomography (CT) reconstruction showed the healing of the mandibular bone 6 weeks after surgery (Figure 1). The osteotomy gap was no longer visible on the corresponding histologies and therefore confirmed the integrity of the mandibular bone. The mandible of the reference animal – however – was not healed as the titanium screws had disengaged from their locking positions.

For the performance study, the animal breed was changed from Göttingen to Yucatan minipigs due to better availability of the latter in North America. Four out of the seven animals had to be

sacrificed within two months as the mandibles were not healing. Only three animals could be kept for the planned duration of 9 months to study the other implantation sites [1, 2] which included orbit, zygoma and ribs.

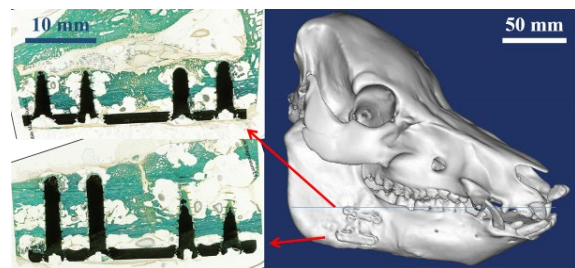


Fig. 1: 3D CT reconstruction of the bone of a Göttingen minipig skull 6 weeks after a complete osteotomy of the mandible and osteosynthesis with coated magnesium plates and screws (right). Histologies of the corresponding mandible bone tissue with implants (left, red arrows).

DISCUSSION & CONCLUSIONS: The effects of the change of miniature pig breed were underestimated. With a weight of 70 – 93 kg, the female Yucatan's were heavier than the Göttingen minipigs (~50 kg). The increased weight went along with more massive mandibles, larger masseter muscles and presumably increased biting force. As a consequence, the performance of human-sized magnesium implants could not be assessed as some of the reference titanium implants failed as well.

Conclusion: The breed of miniature pigs can have a decisive effect on the transferability of the used animal model.

REFERENCES: ¹ B. Schaller, N. Saulacic, T. Imwinkelried, S. Beck, et al. (2016) *J Cranio-Maxillofac Surg* 44(3): 309-317. ² B. Schaller, J.P. M. Burkhard, M. Chagnon et al. (2018) *J Oral and Maxillofac Surg* 76(10): 2138-2150.

ACKNOWLEDGEMENTS: The authors thank the teams from Switzerland and Canada involved with the surgeries and data analysis.

Synthetic composite matrix for dental bone regeneration

L Kind¹, U Pieleš¹

¹*Life Sciences/Institute for Chemistry and Bioanalytics, University of Applied Sciences and Arts Northwestern Switzerland (FHNW), Muttenz, CH*

INTRODUCTION: Dental implants proved to be nowadays a reliable technology for dental prosthesis. Despite their obvious advantages they often require bone augmentation followed by regeneration of bone structure, to achieve a solid anchoring of the implant in the jaw. Usually, a bone substitute combined with a collagen membrane to regenerate the bone is used, which is a time-consuming task for dentist and patient. To simplify this procedure and to improve the quality of bone, a fully synthetic, injectable interconnecting biomimetic matrix will be developed. The new approach combines self-assembling peptide P11 (SAP) with Calcium Phosphate (HAP) granules, forming a dense interconnecting network, which fosters the nucleation and spacial growth of hydroxyapatite crystallites [1, 2, 3]. The SAP-characteristics will support the natural mineralization process resulting in interconnection of the HA-granules and also to the lesion-borders and therefore forming a stable 3D-structure, stabilizing the gap in the jaw and leading to faster bone growth and reconstruction. This approach will minimize the classic bone reconstruction process in dental implantology.

METHODS: A range of stable synthetic matrices are developed by combining A) HAPs and B) SAPs of the P11 family in different ratio. Therefore, the optimal conditions for the combination procedure (buffer, pH-conditions, concentration) were identified. The resulting composite materials were analysed by scanning electron microscopy (SEM) (Fig 1) and transmission electronic microscopy (TEM) to state on homogeneity and connectivity of HAPs within the SAP-network. The possible exclusion criteria of composite materials such as the HAP precipitation is observed over a certain period of time.

Subsequently, a selection of potential HAP/SAP composite materials, are tested regarding their ability and time rate of Ca-nucleation and mineralization.

RESULTS: Intensive research reveal that the SAP form a dense interconnecting 3D-network in pH 6.5, which fosters the nucleation and spatial growth of hydroxyapatite crystallites from saturated hydroxyapatite solution. The

designed HAP/SAP formulation (2:1; 1:1; 1:2) showed a good distribution and HAP granules integration.

The addition of HAP to the SAP matrix in the mentioned ratio does not prevent self-assembling.

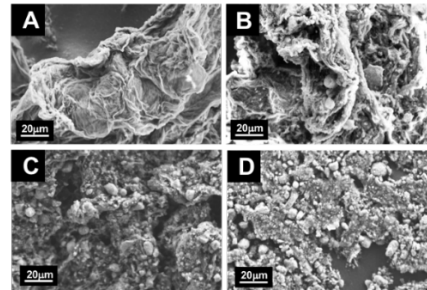


Fig. 1: SEM images of A: P₁₁-4 reference; B: P₁₁-4 to HAP ratio (2:1); C: (1:1) and D: (1:2)

DISCUSSION & CONCLUSIONS: This synthetic system, combining an innovative 3D-matrix made of SAP hydrogel and HAP, showed promising results relating to the construction and stability of the composite matrix. Like that, this system has the potential to add a volume stability to the bone defect due to its viscoelastic properties and mechanical stability.

From preliminary research it is known that the SAP-network provides a matrix for osteoblast and simultaneously preventing the ingrowth of fibroblasts, which is ideal for guided bone regeneration process. This will enhance the bone reconstruction, leading to a faster healing process.

For simple application, the matrix will be freeze-dried in a syringe and dissolved when needed.

REFERENCES: ¹R.P. Davies, A. Aggeli, N. Boden, McLeish TC, Nyrkova IA, Semenov AN. (2009) *Adv. chem. engin.* 35: 11-43. ²F. Koch, M. Müller, F. König, N. Meyer, J. Gattlen, U. Pieleš, K. Peters, B. Kreikemeyer, S. Mathes, S. Saxer (2018), *R. Soc. open sci.*5:171562. ³L. Kind, S. Stevanovic, S. Wuttig, S. Wimberger, J. Hofer, B. Müller, and U. Pieleš, (2017) *J. Dental Res.*96: 790-797.

ACKNOWLEDGEMENTS: The authors would like to thank Aargau Research Fond for providing financial support and credentis AG for scientific support to this project.

Raman spectroscopy-based quality controls for tissue engineered cartilage

L Power¹, A Barbero², I Martin^{1,2}

¹ Department of Biomedical Engineering, University Hospital Basel, CH

² Department of Biomedicine, University Hospital Basel, CH

INTRODUCTION: We are developing tissue engineered cartilage grafts to treat articular cartilage defects using autologous nasal chondrocytes [1] in an ongoing phase II clinical trial. Current methods to assess the quality of engineered tissues are destructive, eliminating the possibility of monitoring grafts continuously and only allows for the assessment of a small part of the graft, which may not be representative of the overall quality. Raman spectroscopy, a method that measures the chemical composition of materials, has the potential to comprehensively and nondestructively characterize engineered cartilage.

METHODS: Native nasal cartilage biopsies were measured with Raman spectroscopy. Nasal chondrocytes were isolated from the biopsies, expanded, seeded onto 3D collagen scaffolds, cultured for up to two weeks in chondrogenic conditions, and measured with a Raman spectrometer. Histological safranin O staining and biochemical quantification of proteoglycans, an important component of cartilage, were performed on the samples and the results correlated with the Raman spectra using statistical learning methods.

RESULTS: The high and low quality native biopsies could be distinguished with a sensitivity of 90% and specificity of 88%. During the two-week process of engineering cartilage, the Raman spectra of the grafts became more similar to the native cartilage spectra. Semi-quantitative histological scores based on the staining intensity and cell morphology of the engineered

cartilages (the highest quality corresponds to a maximum score of six) could be predicted from the Raman spectra with a model using LASSO variable selection and multiple linear regression (Fig. 1).

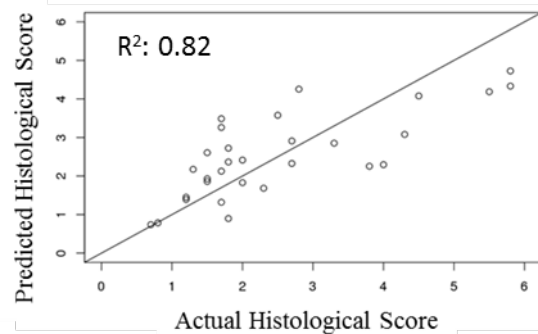


Fig. 1: The quality of the final engineered cartilage graft could be predicted from the Raman spectra.

DISCUSSION & CONCLUSIONS: We show that Raman spectroscopy could be used for nondestructive quality controls to assess the starting materials and final graft quality of tissue engineered cartilage – ensuring product quality and facilitating regulatory compliance.

REFERENCES: ¹ M. Mumme, A. Barbero, S. Miot, A. Wixmerten et al. (2016) *Lancet*, **388**: 1985.

ACKNOWLEDGEMENTS: This work has received funding from the European Union's grant agreement No. 681103 (BIO-CHIP, www.biochip-h2020.eu).

Biodegradable, cytocompatible, antibacterial: Electrospun wound dressings of Ga-PPIX-functionalised P4HB

A Müller¹, C Fessele¹, G Fortunato², RM Rossi², K Maniura-Weber¹,
Q Ren¹, M Rottmar¹, AG Guex^{1,2}

Empa, Swiss Federal Laboratories for Materials Science and Technology, ¹Laboratory for Biointerfaces and ²Laboratory for Biomimetic Membranes and Textiles, St. Gallen, Switzerland

INTRODUCTION: Broadband administration and over-use of conventional antibiotics dramatically contributed to progressive antibiotic resistance, demanding for the development of alternative treatment strategies. Metal ions, derived from copper, zinc or gallium, gained increasing interest as antimicrobial agents [1]. Embedded within a wound dressing, salts or complexes of these metals can provide local and prolonged antibacterial activity within the wound bed. Here, we are reporting on the development and evaluation of electrospun membranes of poly(4-hydroxy butyrate) (P4HB), functionalised with gallium that was complexed in a protoporphyrin ring (Ga-PPIX).

METHODS: P4HB was produced in *E. coli*, extracted with chloroform and purified by repeated precipitation in methanol [2]. The molecular weight was characterised by gel permeation chromatography (GPC). To produce antimicrobial membranes, Ga-PPIX was added to the P4HB solutions at concentrations of 100 μ M or 50 μ M and electrospun with a custom built device [3]. Ga-PPIX-functionalised membranes were then evaluated for their antibacterial activity in cultures of *S. aureus*. Further, the cytocompatibility was investigated by first culturing human dermal fibroblasts (HDF) in Ga-PPIX-supplemented media to assess concentration-dependent effects on cell viability. Subsequently, HDF were seeded on electrospun membranes and cell metabolic activity, proliferation rate, and morphology were assessed after 1, 4 and 7 days.

RESULTS: GPC analysis of biosynthesised P4HB revealed a molecular weight of $1.41 \pm 0.13 \cdot 10^6$ g \cdot mol⁻¹ (with a PDI of 1.74 ± 0.16). P4HB solutions were successfully electrospun into membranes with homogeneous fibres, both for pristine P4HB solutions and Ga-PPIX supplemented membranes (Fig. 1A). Mean fibre diameters were 0.64 ± 0.1 μ m and 0.67 ± 0.13 μ m, respectively. In a disc diffusion assay with *S. aureus* cultures, a Ga-PPIX concentration-dependent inhibition zone could be observed (Fig. 1B). Quantification of CFU reduction on

the membranes is currently under investigation. Ga-PPIX at concentrations of 50 μ M in culture media or higher reduced cell metabolic activity, while all other conditions resulted in metabolic activities of >80% relative to the control group. Cell metabolic activity as well as DNA content of HDFs seeded directly on GaPPIX membranes were comparable to pristine P4HB. After 7 days, a homogeneous monolayer was formed (Fig. 1C).

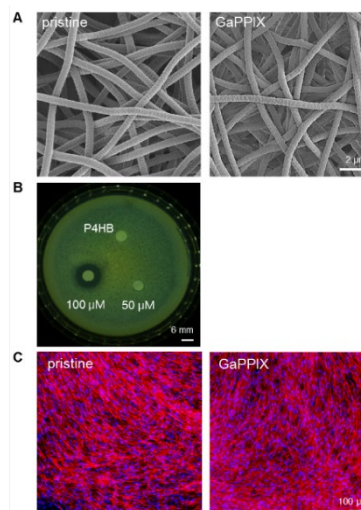


*Fig. 1: A) Scanning electron microscopy (SEM) images of electrospun fibres. B) Inhibition zone of Ga-PPIX-loaded or pristine fibres on *S. aureus*. C) Confocal laser scanning microscopy image of HDF cultured on the membranes for 7 days (100 μ M Ga-PPIX). (red=actin, blue=nuclei).*

DISCUSSION & CONCLUSIONS: Our results provide a proof of concept for the development of a highly cytocompatible, antimicrobial membrane. We are confident that this approach has the potential to contribute to alternative antimicrobial strategies for the treatment of skin wounds.

REFERENCES: ¹R.J. Turner et al. (2017), *Microb Biotechnol*, **10**:1062-1065. ³S. Hein et al. (1997), *FEMS Microbiol Lett*, **153**:411-418. ³A.G Guex et al. (2012) *Acta Biomater* **8**:1481-1498.

Human cell-based engineered tissues induce angiogenesis in healthy rat hearts

L Gili Sole¹, M Mytsyk¹, G Cerino¹, G Isu¹, M Grapow¹, F Eckstein¹, A Marsano¹

¹ Department of Biomedicine and Surgery, University of Basel, Switzerland

INTRODUCTION: Current mesenchymal stem cell (MSC)-based therapies are considered a promising angiogenic strategy to restore the micro-vascularization upon myocardial infarction (MI). The implantation of a cell sheet onto the epicardium resulted to greatly improve the cell engraftment compared to intramyocardial cell injections [1], as well as improved angiogenesis following MI. Contrary to other MSC sources, human adipose tissue-derived stromal vascular fraction (SVF) is a heterogeneous population which contains vascular cells, besides mesenchymal stromal. Previous results showed that SVF cells increase their angiogenic potential following the organization in 3D engineered tissues generated under dynamic condition [2]. Compared to statically generated constructs, 3D culture under direct perfusion promoted 1. *in vitro* growth and organization of endothelial cells and pericytes, and 2. the *in vivo* ingrowth of vessels within the engineered constructs upon implantation in an ectopic rat model [2]. In this study, we hypothesized that the dynamically engineered tissues accelerate their vascularization and that they might also function as delivery system of pro-angiogenic factors inducing angiogenesis also in the surrounding healthy myocardium compared to statically generated constructs.

METHODS: Human adipose tissue-derived SVF cells were cultured on 3D collagen sponges (discs of 8mm diameter and 3mm thickness) either in perfusion-based bioreactors (3mL/min) or in static condition for 5 days. Angiogenic potential (i.e. Vessel Length Density (VLD)) and human cell survival were investigated upon implantation in healthy nude rat hearts after 3 and 28 days.

RESULTS: After 3 days of implantation, the VLD was superior in the perfusion-based SVF patches (not statistical difference). After 28 days *in vivo* instead, perfusion-based patches were significantly better vascularized compared to statically generated constructs (Fig.1). The myocardium underneath the perfusion-based patch also showed an increase in the vessel length density as compared to static condition

(Fig.1). The number of implanted human cells increased in perfusion-based constructs after both 3 and 28 days *in vivo*.

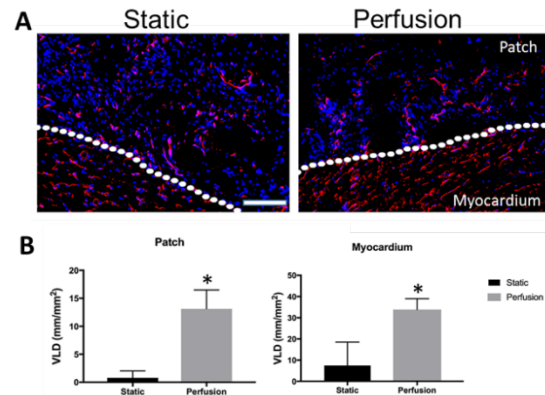


Fig. 1: (A) Immunofluorescence staining for PECAM-1 (red) of constructs generated by SVF cells in static- and perfusion-based culture after 28 days *in vivo*. Nuclei stained with DAPI (blue). Dotted line defines the boundary between healthy myocardium and patch. Scale bar=50 μ m. (B) Quantification of vessel length density (VLD) in the patch of static or perfusion-based constructs and in the underneath myocardium after 28 days *in vivo*. $p < 0.05$. $N \text{ donor} = 1$.

DISCUSSION & CONCLUSIONS: In this study, the healthy heart model was selected to assess the angiogenic potential of the proposed treatment without any other confounding cell processes (e.g. inflammation, wound healing process, fibrosis). Future investigations aim to assess the repair/angiogenic potential of the perfusion-based SVF-patches in a chronic ischemic heart model.

REFERENCES: ¹ H. Hamdi, et al. (2011) *Epicardial adipose stem cell sheets results in greater post-infarction survival than intramyocardial injections*, Cardiovasc Res **91**:483–491. ² G. Cerino (2017) *Engineering of an angiogenic niche by perfusion culture of adipose-derived stromal vascular fraction cells* Sci Rep **27**;7(1):14252.

Engineering clinical-grade β -cell tissues for diabetes treatment

G Born¹, P Saxena², MG Muraro¹, A Scherberich¹, M Fussenegger², I Martin¹

¹Department of Biomedicine, University of Basel and University Hospital of Basel

²D-BSSE, ETH Zürich, Basel

INTRODUCTION: Diabetes mellitus (type 1), affecting at least 415 million people worldwide, results from a loss of pancreatic insulin-producing β -cells. However, all current cell-based diabetes therapies are depended on transplantation of non-autologous cadaveric islets and typically suffer from donor scarcity, compatibility and variability in graft quality. A way to solve these issues is to engineer autologous patient cells that act like healthy pancreatic β -cells and re-implant them. Despite the availability of engineered insulin producing pancreatic like cells for nearly 20 years, the step from the pancreatic cell culture to a functional tissue remained difficult and ineffective due to the high energy consumption and sensitivity of insulin producing cells. We utilized the stromal vascular fraction (SVF) of adipose tissue cultured under medium perfusion to form an environment which has strong vasculogenesis promoting features and might be suitable for β -cells growth, survival, and function.

METHODS: We used mesenchymal stem cells (MSCs) from human adipose tissue, which had been reprogrammed into induced pluripotent stem cells (iPSC) by mRNA transfection (iPSC technology) [1]. By a subsequent 20-day differentiation protocol, these iPSCs (day 0) can be programmed into endodermal cells (day 5), pancreatic progenitor cells (PPCs)(day 12) as well as β -cells (day 20) [2]. Bioreactor chambers with direct perfusion of medium through the culturing matrix are used to overcome the diffusion barrier, the limiting factor for tissue size. Before seeding the pancreatic cells in the bioreactors, SVF cells are cultured to modify commercial scaffolds into living matrices suitable for β -cells and their progenitors. Besides making fast integration in vivo possible, the SVF also form a prevascularization [3], which rapidly develops into a functional support for the β -cells, once in vivo.

RESULTS: So far, the experiments had three aims. First, to test the possibility to 3D culture iPSCs under perfusion on a scaffold, second the effect of co-culturing iPSC derived cells with SVF cells and third estimate the in vivo

pancreatic tissue formation. Real-time PCR analysis of the sorted endodermal cells (day 5), harvested from digested scaffolds after (co-)culturing, showed that iPSC direct cell contact with SVF cells in a perfusion bioreactor system may improve the differentiation towards endodermal lineage (first stage of pancreatic differentiation). Moreover, iPSCs differentiated in the medium in which SVF cells were cultured before, have significantly increased viability compared to PPCs cultured in standard differentiation medium. Finally we proved the existence of pancreatic cells in highly vascularized co-culture constructs in vivo after 3 month.

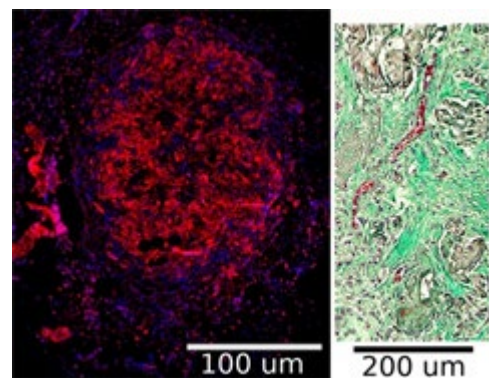


Fig. 1: Co-culture of SVF and pancreatic cells after 3 month in vivo. The left side is an antibody staining, the nuclei are blue, NKX6.1 (β -cell marker) is red. The right side is a Trichrome staining, with clearly visible vascularization.

DISCUSSION & CONCLUSIONS: SVF can support iPSCs survival and differentiation. The perfusion system in combination with the SVF co-culture allows to obtain a tissue construct with higher engraftment potential. Overall, the system might be a new more efficient approach for pancreatic islet transplantation.

REFERENCES: ¹Heng, Boon Chen (2013) *Metabolic Engineering*. ²Saxena, Pratik (2016), *Nature Communications*. ³ Agnes S, Klar (2016), *Pediatric Surgery International*.

Stiff synthetic modular hydrogels foster functional expansion of human hematopoietic stem and progenitor cells

Q Vallmajó-Martin^{1,2}, V Lysenko³, D Alpern⁴, B Deplancke⁴, A Theocharides³, M Ehrbar¹

¹ Laboratory for Cell and Tissue Engineering, Division of Obstetrics, University Hospital Zürich, CH. ² Laboratory of Stem Cell Bioengineering, Institute of Bioengineering, EPFL, Lausanne, CH. ³ Laboratory of experimental hematology, Division of Hematology, University Hospital Zürich, CH. ⁴ Laboratory of Systems Biology and Genetics, Institute of Bioengineering, EPFL, Lausanne, CH

INTRODUCTION: Sufficient numbers of hematopoietic stem and progenitor cells (HSPCs) needed for bone marrow transplantations remains a major challenge in medicine today. HSPCs grown *in vitro* rapidly lose their regenerative capacity likely due to the lack of niche-derived signals comprising molecular, cellular and mechanical components [1]. Identification of critical hematopoietic niche components necessitates the generation of more tractable *in vitro* platforms. An attractive solution is to employ a blank biomaterial that modularly can be decorated with different moieties known to be present in the niche *in vivo*. This sophisticated approach allows to assess the individual contributions of each parameter on HSPC fate decisions. Here, we engineered a previously reported synthetic poly(ethylene glycol)-based (TG-PEG) hydrogel [2] to recapitulate this hematopoietic stem cell niche.

METHODS: *In vitro* culture of human umbilical cord blood-derived CD34+ cells was established for different 3D biomaterials including natural hydrogels -such as collagen and fibrin- and functionalized biomimetic polyethylene glycol (PEG) hydrogels. Stiffness, initial seeding density, presentation of specific moieties, co-culture with and without mesenchymal stem cells (MSCs) and combinations of the above approaches was established. Success was determined via FACS analysis, cell counting, CFUs potential and imaging. Ultimately, HSPCs cultured in selected conditions were transplanted to irradiated NSG mice to evaluate their regenerative potential *in vivo*.

RESULTS: The effect of stiffness, cell-adhesion and degradability on hHSPCs proliferation and stemness capacity was assessed. Surprisingly, stiffer gels exhibited higher percentage of phenotypically defined-HSPCs and HSCs as seen by flow cytometry

analysis. Furthermore, these cells also exhibited a higher colony formation (CFU) capability to differentiate into the different blood lineages. We next validated the role on human HSPCs of several niche ligands including cell-cell and cell-matrix adhesion moieties, as well as growth factors by incorporating them into the TG-PEG-backbone. Intriguingly, Notch signaling pathway-related ligands consistently increased the percentages of both HSPCs and HSCs over other populations. Finally, upon transplantation into NSG mice, HSPCs encapsulated in TG-PEG hydrogels containing the Jagged 1-ligand could only reconstitute the hematopoietic system short-term -up to 4 months, while HSPCs retrieved from stiff hydrogels engrafted up to 6 months and were found in abundant numbers in the host bone marrow niche. Taken all together corroborates that truly functional HSCs are maintained in stiff TG-PEG hydrogels.

DISCUSSION & CONCLUSIONS: Hydrogel conditions including stiffness, cell-adhesion sites, proteolytic degradability and bioactive moieties were screened to optimize conditions for hHSPCs culture *in vitro*. Findings suggest strong roles for hydrogel stiffness in hHSPC stemness maintenance most probably by balancing pro-proliferative and anti-differentiative effects. Ongoing deeper analysis based on RNA sequencing and proteomics aim at elucidating the effect of these culture conditions on HSPC stemness potential. This minimalistic human bone marrow analogue presents a potent tunable platform to use in the discovery of critical hematopoietic stem cell niche factors.

REFERENCES: ¹ S.J. Morrison, D.T. Scadden (2014) *Nature* 505:327-334. ² M. Ehrbar et al. (2007) *Biomaterials* 28:3856-66.

ACKNOWLEDGEMENTS: This work was funded by the Swiss National Science Foundation grant 153316.

Spatially orchestrated micro-vessels networks via acoustic waves cell patterning

T Serra¹, D Pellicciotta¹, V Basoli¹, E Della Bella¹, AR Armiento¹, RG Richards¹, M Alini¹, D Eglin.¹

¹ *AO Research Institute Davos, Davos, CH*

INTRODUCTION: Cell patterns are important for studying morphogenesis, unravelling biophysical mechanisms, and in the development of novel tissue engineering approaches. Surface acoustic wave (SAW) technologies, based on a Faraday wave principle, enable the generation of spatially orchestrated particulate systems (cells, spheroids, inorganic aggregates). The pattern can be tuned on demand by varying a set of parameters, such as sound frequency, amplitude, and chamber shape. Here we study how the use of a SAW-based technology, named 3D sound induced morphogenesis (3D-SIM), allows the generation of spatially-controlled particulate systems such as cells, spheroids or bioactive particles [1]. 3D-SIM has also been used to drive the organization of functional microvascular networks.

METHODS: Patterns composed of calcium phosphate particles (three different sizes: 32-75 μm , 125-250 μm and 250-500 μm) were tested. As hydrogels: i) gelatin methacryloyl (GelMA, 5%w/v) / Irgacure 2959 solution in PBS and ii) fibrin gel (fibrinogen-thrombin, SIGMA) were used. Finite element analysis (FEA), particle dynamic simulation, was conducted to properly select cell pattern shapes. Primary human mesenchymal stem cells (hMSCs) and human umbilical vein endothelial cells (HUVECs) were used to generate the microvessel networks. Briefly, spheroids were generated (hMSCs:HUVECs 1:1, 2×10^5 cell/ml in low-adherent petri dishes) and patterned at a frequency of 80Hz and low amplitude for 15s in fibrin gel (2.5 mg/ml of fibrinogen, 0.333 IU/ml of thrombin). Morphological analysis via optical and confocal microscope was performed. Endothelial cell sprouting, and vessel formation were imaged until day 10.

RESULTS: The acoustic waves can modulate cells/particulates systems organization in a fluid over an area of 28 cm^2 in less than 15 seconds. This process is applicable to a wide range of off-the-shelf gelling biomaterial matrices. Layers composed by several combinations of hydrogel and cells/bioactive particles were generated and used as matrices. As well, spheroids pattern morphology was confirmed by FEA investigation. 3D constructs were created by staking layers of patterned cells embedded in hydrogel matrices. Live/Dead assay staining of cells and spheroids patterns embedded in the fibrin gel, at 1 and 4 days, showed high cells viability (>95%). This confirmed that 3D-SIM is a mild fabrication process. Circular concentric patterns of HUVECs with 1 mm distance were produced. HUVECs after 6 days formed interconnecting networks forming a meso and micro scale organization.

DISCUSSION & CONCLUSIONS: 3D-SIM is an affordable and user-friendly technology to create 3D cell models in a time-effective manner, with sufficient and controlled spatial complexity, retaining high cell viability. Hierarchically shaped vessels with a multiscale organization (meso-micro scale), obtained via 3D-SIM, can be integrated into cm-scale fluidic device where perfusion can be performed in a reproducible manner with a controlled flow rate.

REFERENCES: ¹T. Serra, D. Eglin, M. Alini. Surface Acoustic Wave (SAW) 3D Printing Method - Nr. 01058/17

ACKNOWLEDGEMENTS: The authors would like to thank BRIDGE programme (SNSF-Innosuisse) for providing financial support to this project (SNSF grant number: 20B1-1_178259).

Enzymatically cross-linked cationic arginine-chitosan hydrogels for cartilage tissue engineering

I Berg¹, M Lee¹, M Zenobi-Wong¹

¹ Tissue Engineering and Biofabrication, ETH Zürich, Zürich, CH

INTRODUCTION: The limited self-repair ability of cartilage has prompted great efforts to develop engineered materials such as injectable and biodegradable hydrogels to assist tissue regeneration. Here we propose a novel enzymatically cross-linked arginine-chitosan hydrogel for cartilage repair. Given the high negative charge of cartilage, we hypothesize that the cationic, *in situ* polymerizing chitosan derivative could increase tissue infiltration and thus allow for cross-linking within the tissue, potentially leading to strong adhesion (Fig. 1).

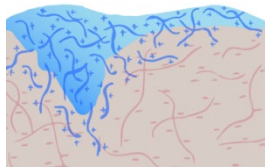


Fig. 1: Infiltration of a cationic *in situ* polymerizing hydrogel (blue) into negatively charged cartilage ECM (brown).

METHODS: Transglutaminase (TG) cross-linkable arginine-chitosan polymers (ArgChi-TG) were synthesized by conjugation of both arginine and a linker molecule to chitosan by EDC-mediated amide bond formation, followed by a Michael Addition reaction to conjugate TG substrate peptides to the linker molecule [1,2]. The ArgChi-TG polymers were subsequently crosslinked using FXIIIa TG, and the gelling kinetics and stiffness of the hydrogels were characterized using a rheometer. Tissue infiltration was assessed by incubation of bovine articular cartilage explants in FITC-labelled chitosan and arginine-chitosan solutions and subsequent imaging. Cell compatibility was assessed by compression testing and live/dead staining of bovine articular chondrocytes (1×10^7 cells/mL) encapsulated in 3% ArgChi-TG hydrogels, cultured over three weeks.

RESULTS: FXIIIa TG-mediated gelation of ArgChi-TG hydrogels was achieved within a few minutes and a final stiffness of approximately 200 Pa in 2% and 700 Pa in 3% hydrogels was obtained (data not shown).

Arginine-chitosan, compared to unmodified chitosan, did not only provide a larger range of

solubility necessary for polymer modification, but may also infiltrate more efficiently into bovine cartilage tissue and may thereby lead to formation of a polymer network across the tissue-hydrogel border, contributing to adhesion (Fig. 2).

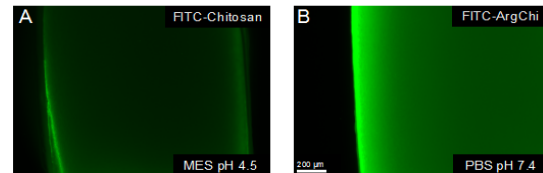


Fig. 2: Chitosan and arginine-chitosan infiltration into bovine articular cartilage explants.

Live/dead staining of ArgChi-TG-encapsulated bovine chondrocytes showed an average viability of 76% over the duration of 21 days in culture. An increase in compressive modulus of approximately 400% suggests the deposition of ECM by the encapsulated chondrocytes (Fig. 3).

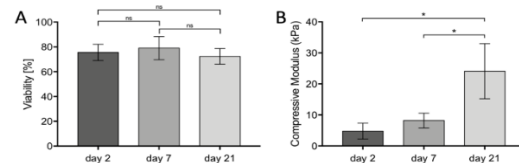


Fig. 3: Viability of bovine chondrocytes encapsulated in 3% ArgChi-TG hydrogels (A) and hydrogel compressive modulus (B).

DISCUSSION & CONCLUSIONS: Cationic ArgChi-TG hydrogels can support cell survival and the increase in compressive modulus over time suggests production of ECM. Our findings may provide novel tools for clinical applications involving tissue infiltration and adhesion or drug delivery, leading to less invasive and more sustainable repair of cartilage lesions.

REFERENCES: ¹ S.P. Baker, W. Wiesmann, R. Shannon (2012), Chitosan-derivative compounds and methods of controlling microbial populations, *U.S. Patent* No. 8,119,780. ² N. Broguiere, L. Isenmann, M. Zenobi-Wong (2016) Novel enzymatically cross-linked hyaluronan hydrogels support the formation of 3D neuronal networks, *Biomaterials* **99**, 47–55.

Bioprinting of Osteochondral Grafts

F Roth¹, P Fisch¹, M Zenobi-Wong¹

¹ *Tissue Engineering and Biofabrication Laboratory, ETH Zürich, Zürich, CH*

INTRODUCTION: Articular cartilage defects are mainly caused by daily wear and tear and can lead to the progression of osteoarthritis. The reduced healing capacity of articular cartilage demands surgical interventions as mosaicplasty to prevent this. In this procedure osteochondral grafts are punched out from other articular surfaces and placed into drilled holes in the lesion. Limitations lie within the limited availability of sacrificial tissue and donor-site morbidity with further complications. Additional demands arise as mosaicplasty is a second treatment after failed microfracture or autologous chondrocyte implantation [1]. Therefore, the development of tissue-engineered osteochondral grafts is an urgent medical need.

METHODS: Osteochondral grafts were bioprinted containing human auricular chondrocytes in the cartilage bioink, cultured for 21 days and tested for viability, mechanical development and matrix deposition. Adhesion of bone and cartilage part was ensured with an intertwining in between with alternating strands of boneink and cartilage bioink. A calcium phosphate cement based boneink (Innotere, Germany) was used for the bone part. and the following bioinks for the cartilage part:

HATG bioink [1]: 1.5% transglutaminase cross-linkable hyaluronan (HATG), 1.5% hyaluronic acid, 2% sNAG nanofibers

HATGALG bioink: 0.5% HATG, 0.25% sodium alginate, 1.5% hyaluronic acid, 2% sNAG nanofibers

The *HATGALG bioink* was developed with focus on better adhesion to the boneink and similar rheological properties than the *HATG bioink*. Cylindrical samples (4mm x 1mm) were casted of both bioinks with human auricular and human articular cells and tested for viability, mechanical development and matrix deposition during 63 days.

RESULTS: The addition of alginate in the *HATGALG bioink* enhanced the adhesion to the boneink. The HATG concentration was lowered and a storage modulus after cross-linking similar to the HATG bioink was achieved. In the cylindrical samples human auricular cells showed higher

viability after 21 days and much higher compressive strength after 63 days than the articular cells with more than 1MPa in the *HATGALG bioink* samples. Higher amounts of GAGs, collagen type II and a more homogeneous matrix deposition were found in auricular chondrocyte cylindrical samples in histology. Osteochondral grafts were successfully printed and cultured with both bioinks. The cell viability was higher than 78% after 7 and 21 days in all conditions. Lower values were measured, next to the intertwining in the middle of the cartilage part (>64%). Less matrix deposition was seen compared to the cylindrical samples and compressive modulus was about 5 to 10 times lower depending on the bioink at day 63.

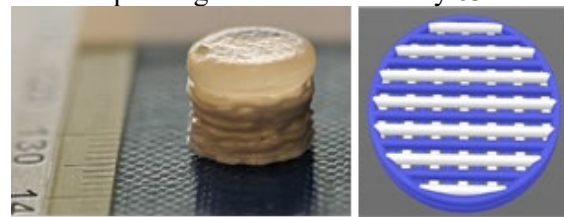


Fig. 1: The osteochondral graft on the left side was bioprinted with multi head extrusion. On the right the intertwining between is shown.

DISCUSSION & CONCLUSIONS: A first generation of tissue-engineered osteochondral grafts for the treatment of full-thickness cartilage defects also affecting the subchondral bone were presented. Bioprinting was used for fabrication because it allows osteochondral graft production for the treatment of different defect shapes and sizes. The presented osteochondral grafts serve as a basis for further research. The *HATGALG bioink* could be a promising material for future cartilage engineering applications. Encapsulated in cylindrical samples of this bioink human auricular chondrocytes formed new cartilage with structural and mechanical similarities to native tissue. Tissue formation was less in the bioprinted osteochondral grafts which demand further analysis.

REFERENCES: ¹Steven B Abramson. *Cartilage Biology. NYU School of Medicine - Division of Rheumatology*, 14:500, 2007. ²Philipp Fisch, Nicolas Broguiere, S Finkielstein, T Linder, and Marcy Zenobi-Wong. (in preparation). 2018.

The effect of confinement of β -Tricalcium phosphate granules immersed in SBF on local solution changes

Y Maazouz¹, I Rentsch¹, B Le Gars Santoni¹, B Lu¹, M Bohner¹

¹ RMS Foundation, Bischmattstrasse 12 - Postfach 203 - 2544 Bettlach, SO – CH

INTRODUCTION: The mechanism of calcium phosphate induced intrinsic osteoinduction remains unclear. It is mostly observed with beta-tricalcium phosphate (β -TCP), hydroxyapatite, or their combination but not exclusively [1]. A local decrease in Calcium, Phosphate and pH to sub-physiological levels provoked by the confinement and bioactivity of materials was related to the early stages of material induced ectopic bone formation [1]. Understanding the effect of confinement and bioactivity through pH, Calcium and Phosphate measurements by simulating the local microenvironment created by a bone graft is of paramount importance to better understand β -TCP's bioactivity and osteoinductivity both reported positively and negatively [2]. The present work addressed these aspects.

METHODS: Particle size (S=fine, coarse), calcium to phosphorus ratio (Ca/P= 1.50, 1.51) Specific Surface Area (SSA: large=4m²/g, small=1m²/g) and (micro) porosity (P= high, low) were varied in a full factorial design to produce 16 types of β -TCP granules with all possible combinations of factors. A two test method was developed: I) Unconfined test: A mass of 0.3g of material was introduced under agitation in 200ml of SSBF and pH was monitored owing to an electrode (Unitrode, Metrohm) every seconds during 22 hours. II) Confined test: a 5cc chamber constituted of 40 μ m mesh (Cell Strainer, BD Falcon) was entirely filled with granules and a 3mm outer diameter pH electrode (Biotrode, Metrohm) was introduced in the center of the granules for the pH to be recorded every second for up to 96h.

RESULTS: The pH changes in the confined and unconfined test differed drastically. Confinement provoked higher variation of pH, and the effect of the varied properties of β -TCP granules on the pH variations were markedly larger. In the unconfined test pH slowly decreased with time. This decrease was attributed to the heterogeneous precipitation of an apatite phase. SEM pictures and solubility calculations confirmed this finding. SSA (p=0.0001) and porosity (p=0.006) significantly influenced the pH decrease kinetics. In the case

of the confined test a pH increase followed by a sharp decrease were observed. The kinetics of the pH increase and subsequent decrease was significantly impacted by the granule size (p=0.001) and the SSA (p=0.007). Granule size did not impact pH changes in the unconfined contrary to the confined test. Furthermore, SSA had an opposite effect in each test, accelerating the pH decrease in the unconfined test while slowing it down in the confined test.

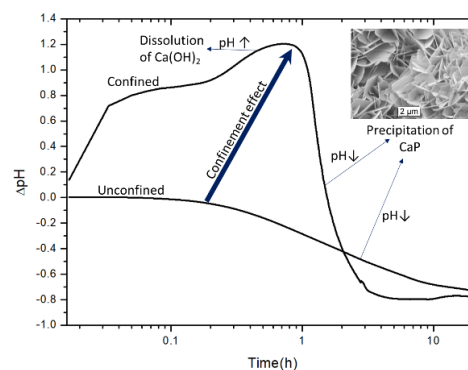


Fig. 1: Sample Δ pH curves showing for the same type of β -TCP granules (Coarse, 4m²/g, high porosity) the effect of confinement on local pH.

DISCUSSION & CONCLUSIONS: Two new bioactivity tests unravelled the substantial pH changes provoked locally by β -TCP granules *in vivo*. The considerable kinetics differences in pH changes and bioactivity that materials with similar compositions exhibited should be taken into account for the design of β -TCP granules. Finally, the present results open up new perspectives towards linking the physicochemical phenomena with intrinsic osteoinduction.

REFERENCES:

- ¹ M. Bohner, & R.J. Miron, A proposed mechanism for material-induced heterotopic ossification. *Mater. Today* **22**, 132–141 (2019).
- ² R. Xin, Y. Leng, J. Chen, & Q. Zhang, A comparative study of calcium phosphate formation on bioceramics *in vitro* and *in vivo*. *Biomaterials* **26**, 6477–6486 (2005).

ACKNOWLEDGEMENTS:

Acknowledges the SNF (grant n°200021_169027).

B.LGS.

Osteoclastic resorption of pure beta-tricalcium phosphate dense ceramics

B Le Gars Santoni¹, M Gallo², T Douillard², C Stähli¹, N Döbelin¹, S Dolder³, S Meille²,
W Hofstetter³, J Chevalier², S Tadier², M Böhner¹

¹ Bioceramics and biocompatibility group, RMS Foundation, Bettlach, CH. ² University of Bern, Department for BioMedical Research, Bern, CH. ³ Université Lyon, INSA Lyon, MATEIS UMR CNRS 5510, Villeurbanne, France

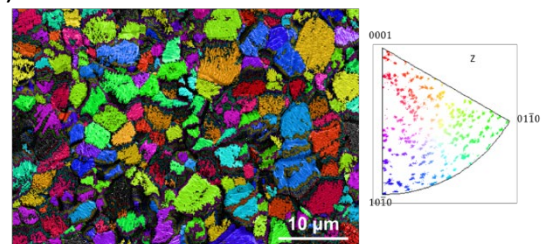
INTRODUCTION: β -tricalcium phosphate ($\text{Ca}_3(\text{PO}_4)_2$; β -TCP) is a promising bone graft substitute due to its chemical similarity to bone mineral, its osteoconductive properties and its osteoclast (OC) mediated resorption [1]. Generally, β -TCP grains resorbed by OC show very oriented “dissolution pits” [2], suggesting a preferential crystallographic orientation for resorption. However, this correlation was not confirmed yet. The aim of this study was to verify that the osteoclastic resorption of β -TCP is a crystallographically-driven process.

METHODS: Pure calcium deficient hydroxyapatite (CDHA) with a Ca/P ratio of 1.50 was precipitated via addition (4 mL/min) of a diammonium hydrogen phosphate solution into a calcium nitrate tetrahydrate solution. The CDHA was converted into β -TCP by a thermal treatment (850°C for 1 hour). Finally, dense β -TCP cylinders were obtained by subsequent powder milling, slip casting and sintering (3 h, 1100°C). Phase purity and content of chemical impurities were measured by X-ray diffraction (XRD) and inductively coupled plasma mass spectrometry (ICP-MS), respectively. OC were derived from osteoclast progenitor cells (OPC) [3] and placed on the β -TCP surfaces for 24 hours. Resorbed β -TCP surfaces were imaged by SEM-SE and orientation of resorbed grains prior and after OC resorption were acquired by electron backscatter diffraction (EBSD) measurements.

RESULTS: The β -TCP cylinders were phase pure and chemically pure (maximum: 30 ppm for Sr). After the resorption by OC, numerous OC resorption tracks were observed microscopically on β -TCP samples. In addition, imaging of resorbed grains showed presence of characteristic “dissolution pits” on their surface. Their analysis with EBSD revealed (fig 1.a) that the crystalline orientation of the oriented pits matched the c-axis of the β -TCP crystal structure (fig 1.b). Also, the grains whose c-axis was oriented nearly normal to the sample surface were more prone to resorption.

DISCUSSION & CONCLUSIONS: SEM-EBSD measurements demonstrated that the resorption of β -TCP is a crystallographically-driven process which preferentially proceeds along the crystallographic c-axis of the β -TCP crystal structure.

a)



b)

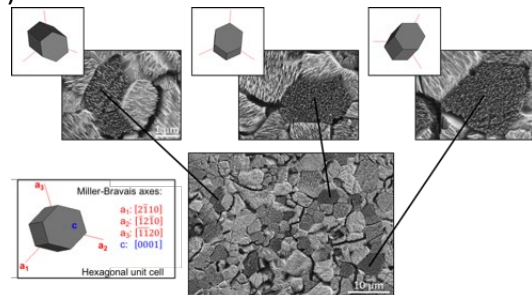


Fig. 1: a. Superposition of SEM image and crystal orientation map derived from EBSD and displayed in Inverse Pole Figure (IPF) colouring according to the Z reference direction (the sample normal) [4]. b. Correlation between dissolution pits and the β -TCP crystal orientation [4].

REFERENCES: ¹M. Böhner, *Materials Today*, 2010;13: 24-30. ²M. Böhner et al., *J. Eur. Ceram. Soc.*, 2012;32:2663-2671. ³ N. Ruef et al., *Bone* 2017; 97: 267-277. ⁴M. Gallo, B. Le Gars Santoni, *Acta Biomaterialia* 2019, <https://doi.org/10.1016/j.actbio.2019.02.045>

ACKNOWLEDGEMENTS: This work was funded by the SNSF grant n°200021_169027 and the European Commission funding of the 7th Framework Program (Marie Curie Initial Training Networks; grant number: 289958, Bioceramics for bone repair).

Magnesium-based bone scaffolds fabricated by Laser Powder Bed Fusion: Microstructure analysis and surface coatings for degradation protection

L Berger¹, F Bär¹, L Jauer², R Schäublin¹, J H Schleifenbaum^{2,3}, J F Löffler¹

¹Laboratory of Metal Physics and Technology, Department of Materials, ETH Zurich, 8093 Zurich, Switzerland. ²Fraunhofer Institute for Laser Technology ILT, Aachen, Germany.

³Digital Additive Production, RWTH Aachen, Germany

INTRODUCTION: In orthopedic surgery, biodegradable metal implants have received considerable attention lately, with magnesium being the most prominent representative. However, the control of its relatively high degradation rates under physiological conditions is a challenge, but can be achieved by appropriate alloying or surface coatings. In addition to controlled degradability, sometimes complex component geometries may be required for implant applications, such as scaffolds for bone regeneration. An open-cell scaffold of appropriate size can stimulate cell ingrowth while structurally supporting the bone. However, such structures are difficult to fabricate with conventional methods, calling for additive manufacturing techniques. Especially promising in this respect is Laser Powder Bed Fusion (LPBF), which can produce such scaffolds of magnesium alloys [1].

METHODS: Samples from the Mg-Y-RE-Zr-alloy WE43 were prepared by LPBF with a single ytterbium fiber laser with a maximum output power of 230W. In a series of constitutional studies, the influence of fluoride, phosphate and hydroxyapatite coating on the resistance to degradation under physiological conditions was investigated. The microstructure was examined with a 200 kV transmission electron microscope with energy dispersive X-ray spectroscopy.

RESULTS: While all three coatings tested showed improved resistance to degradation, it was found that the hydroxyapatite coating had the greatest effect with a slowdown in degradation by about one order of magnitude.

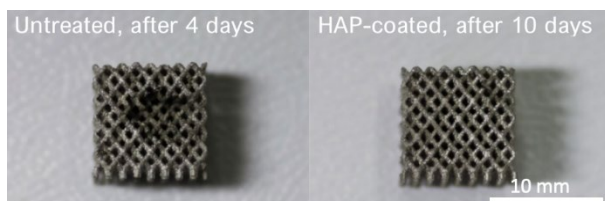


Fig. 1: Comparison of untreated and hydroxyapatite (HAP) coated scaffolds after

immersion in simulated body fluid for 4 days and 10 days, respectively. Degradation is more advanced on untreated specimen, even after shorter immersion time.

The high-resolution microstructural studies showed the presence of various types of incorporated particles and precipitates. Besides randomly distributed yttrium oxide particles, two types of rare earth-rich precipitates were identified: the intermetallic phases Mg_3Nd and $Mg_{41}Nd_5$.

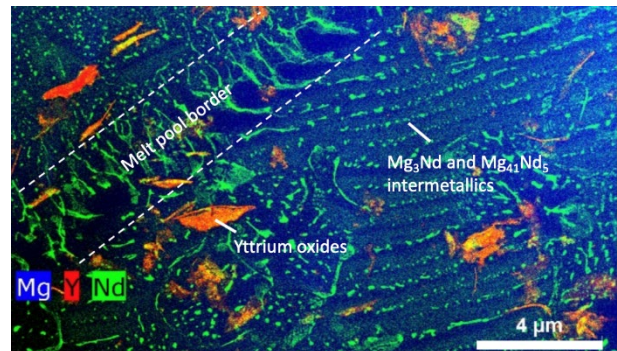


Fig. 2: Microstructure of WE43 synthesized by LPBF.

DISCUSSION & CONCLUSIONS:

Yttrium, originally used in WE43 to form a protective oxide layer on the material surface, was bound in yttrium oxide particles. These particles are believed to be shells from the original powder that were scattered during the material synthesis process. Since less yttrium is available for corrosion protection, it is expected that this will lead to increased degradation rates.

As a possible solution, however, it could be demonstrated that a hydroxyapatite coating significantly improves the corrosion resistance of porous scaffold structures fabricated by Laser Powder Bed Fusion.

REFERENCES: ¹ Jauer, L. et al. Selective Laser Melting of magnesium alloys. *European cells & materials*. 30, pp. 1, (2015).

ACKNOWLEDGEMENTS: We acknowledge ScopeM from ETH Zurich for providing the electron microscope facility and assistance